

Description of the Electron Transport in Submicron GaAs MESFET's  
With the Effective Mobility Including Near Ballistic Transport

Yoshinori YAMADA

Department of Electrical Engineering and Computer Science  
Kumamoto University, Kumamoto 860, JAPAN

ABSTRACT—It has been found that the electron transport in the low-field region under the gate in a 0.25  $\mu\text{m}$  gate GaAs MESFET should not be expressed by the bulk mobility( $\mu_B$ ), but by the effective mobility( $\mu_S$ ) including the near ballistic transport.

SIMULATION RESULTS—The velocity-field(V-F) characteristics in the 0.25  $\mu\text{m}$  gate GaAs MESFET have been evaluated under the gate using the particle simulator with an ensemble Monte Carlo technique(PS), which are shown in Fig. 1. We define the saturation velocity( $\mathcal{V}_S$ ) and the effective mobility( $\mu_S$ ) by  $\mathcal{V}_S=0.8 \mathcal{V}_{\text{max}}$  and  $\mu_S = \mathcal{V}_S/F_S$ , respectively, where  $F_S$  is the saturation field corresponding to  $\mathcal{V}_S$ . The properties of  $\mu_S$  and  $\mathcal{V}_S$  can be successfully expressed as functions of the average gradient of the distribution of electric field(A) in the low field region. Then  $\mu_S$  decreases and  $\mathcal{V}_S$  increases, as A increases(Figs. 2 and 3). These are caused from inertia of electrons in the near ballistic transport. The values of A are estimated by  $A=F_S / \Delta z$ , where  $\Delta z$  is the distance from the source  $n^+$ -n junction to the saturation point. Naturally the increase of A corresponds to that of the drain voltage( $V_D$ ). At  $V_D=1.0 \text{ V}$  ( $A \sim 20 \text{ V}/\mu\text{m}^2$ )  $\mu_S$  is about a half of  $\mu_B$  ( $\sim 6,300 \text{ cm}^2/\text{Vs}$ ). Thus, the dependence of  $\mu_S$  on A is significant.

MODELING—The above properties of  $\mu_S$  and  $\mathcal{V}_S$  can be also predicted by a simple 1D relaxation time approximation(RTA) for a simplified model of a linearly graded distribution of electric field( $F=Az$ ). The V-F characteristics in Fig. 4 and the solid lines in Figs. 2 and 3 are numerically obtained by the RTA. The solid line for  $\mu_S$  excellently agrees with the circles obtained by PS. Figure 5 illustrates a basic difference between the conventional and present models for the V-F characteristics using  $\mu_S$  and  $\mathcal{V}_S$ . It is stressed that the electron transport in the low-field region under the gate should not be expressed by  $\mu_B$ , but by  $\mu_S$ .

We have also derived simple analytical expressions for  $\mu_S$  and  $\mathcal{V}_S$  which are based on the RTA and introduced the expressions into an analytical device model. Fig. 6 shows a comparison between the I-V characteristics obtained by the analytical model(—) and the simulation( $\circ, \bullet$ ).

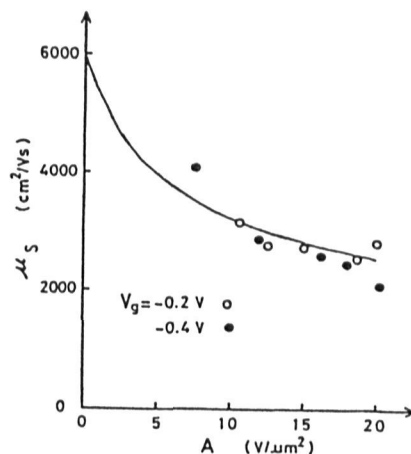
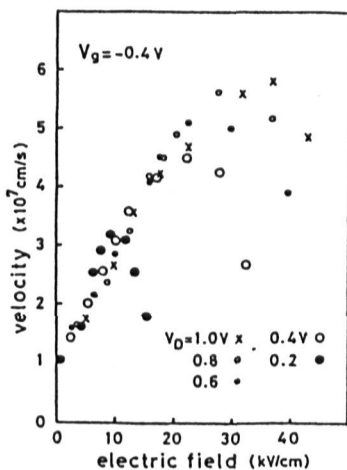
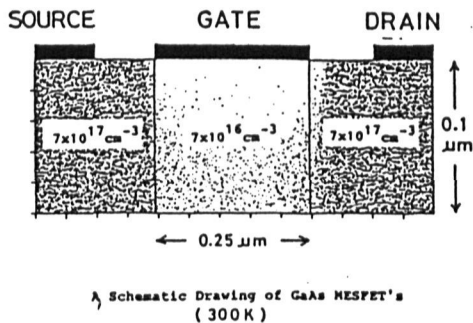


Fig. 1 V-F characteristics

Fig. 2

Dependence of  $\mu_s$  on  $A$ . Circles are obtained by PS and the line by RTA.

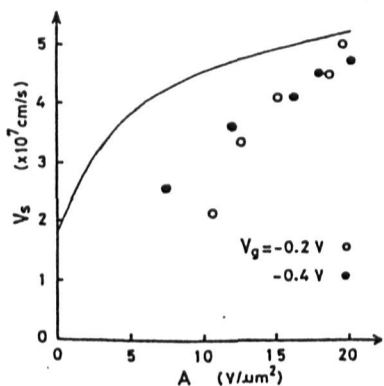


Fig. 3 Dependence of  $v_s$  on  $A$ . The notations are as same as those in Fig. 2.

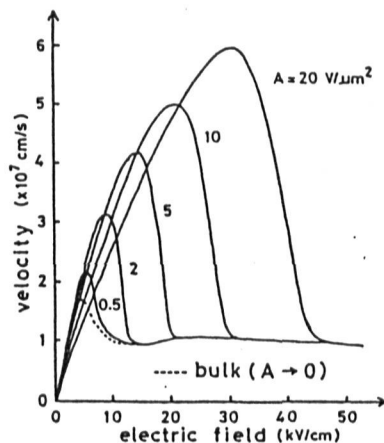


Fig. 4 Velocity-field characteristics obtained from the model distribution of electric field using 1D RTA.

conventional model      present model

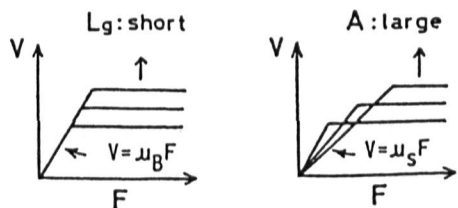


Fig. 5 Schematic drawings of the V-F characteristics using the mobilities and saturation velocity.

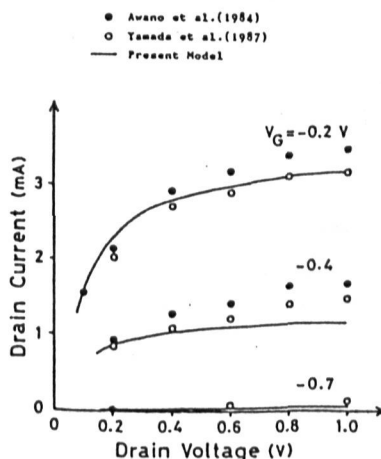


Fig. 6 Current-voltage characteristics.